

LES OF THERMALLY-STRATIFIED LIQUID TURBULENT FLOWS WITH A CHEMICAL REACTION

Ryo Onishi

Department of Mechanical Engineering, Kyoto University
Yoshidahonmachi, Sakyo-ku, Kyoto 606-8501, Japan
ryo@fld.mbox.media.kyoto-u.ac.jp

Takenobu Michioka

Central Research Institute of Electric Power Industry,
Iwado-kita, Iwae-shi, Tokyo 201-8511, Japan
michioka@criepi.denken.or.jp

Kouji Nagata

Department of Mechanical Engineering, Kyoto University
Yoshidahonmachi, Sakyo-ku, Kyoto 606-8501, Japan
nagata@mech.kyoto-u.ac.jp

Satoru Komori

Department of Mechanical Engineering, Kyoto University
Yoshidahonmachi, Sakyo-ku, Kyoto 606-8501, Japan
komori@mech.kyoto-u.ac.jp

ABSTRACT

Two types of reacting liquid turbulence with density stratifications; a mixing layer and grid-generated turbulence, were numerically investigated using large-eddy simulation (LES). The present LES employed the dynamic SGS models for the SGS Reynolds stress and SGS mass and heat fluxes and our SGS model for the chemical reaction source term (Michioka *et al.*, 2001). The LES based on these SGS models was applied to the same stratified reacting liquid turbulent flows as in our recent experiments (Onishi *et al.*, 2003). To examine the applicability of the present LES, the predictions of some turbulence statistics were compared with the measurements by Onishi *et al.* (2003).

The results show that the LES predictions are in good agreement with the measurements and the present LES can accurately estimate buoyancy effects on the diffusive-reactive mechanism in thermally-stratified reacting liquid turbulent flows.

INTRODUCTION

Turbulent reacting liquid flows with density stratifications are often seen not only in industrial reactors but also in environmental water flows with chemical pollutants. It is, therefore, of great importance to investigate the reactive-diffusive mechanism in density-stratified reacting liquid turbulence. In spite of its importance, few numerical studies on the diffusive-reactive mechanism have been conducted in stratified liquid flows because of the high Schmidt number and complicated buoyancy effects.

One of the promising simulation techniques for such flows is the large-eddy simulation (LES) since direct numerical simulation (DNS) cannot be applied to practical reacting liq-

uid flows with the high Schmidt and Reynolds numbers. In the LES, large scale (grid scale: GS) quantities are directly computed, and small scale (sub-grid scale: SGS) quantities are predicted by using SGS models. In order to apply the LES to practical reacting flows with density stratifications, a SGS model for explicitly describing the diffusive-reactive mechanism and buoyancy effects is required. One of the major SGS models has been proposed by Gao and O'Brien (1993). The model is based on the large eddy probability density function (LEPDF) of concentration of chemical species and the LEPDF can be derived from a transport equation of the LEPDF. However, the equation needs a lot of closure hypotheses, so that it takes a high computational cost. Another one is the beta assumed-pdf approximation model by Cook and Riley (1994). But the model is not applicable to liquid turbulence since the SGS concentration variance that is important in liquid turbulence has not been considered.

The above status of SGS modeling has suggested that an effective SGS model which is applicable to reacting liquid turbulence should be developed. Recently we have developed a simple but powerful SGS model based on the β -pdf model in which the SGS concentration variance is considered (Michioka *et al.*, 2001) and we have examined the applicability and reliability of our proposed SGS model by comparing with the measurements in neutral reacting liquid turbulence without density stratification. However, the applicability of our proposed SGS model to reacting liquid flow with stable and unstable density-stratifications has not been confirmed.

The purpose of this study is, therefore, to develop our LES to be applicable to density-stratified reacting liquid flows and to confirm the reliability of the LES by comparing with our measurements (Onishi *et al.*, 2003) in stratified

conditions.

LARGE-EDDY SIMULATION

The governing equations are the continuity equation, momentum, mass and heat conservation equations. Filtered governing equations can be written as

$$\frac{\partial \bar{U}_i}{\partial x_i} = 0, \quad (1)$$

$$\frac{\partial \bar{U}_i}{\partial t} + \bar{U}_j \frac{\partial \bar{U}_i}{\partial x_j} = -\frac{1}{\rho} \frac{\partial \bar{P}}{\partial x_i} + \nu \frac{\partial^2 \bar{U}_i}{\partial x_j \partial x_j} - \frac{\partial \tau_{ij}}{\partial x_j} - \beta g_i (\bar{T} - T_s), \quad (2)$$

$$\frac{\partial \bar{C}_i}{\partial t} + \bar{U}_j \frac{\partial \bar{C}_i}{\partial x_j} = \frac{\nu}{Sc} \frac{\partial^2 \bar{C}_i}{\partial x_j \partial x_j} - \frac{\partial q_{ij}}{\partial x_j} + \bar{\omega}, \quad (3)$$

$$\frac{\partial \bar{T}}{\partial t} + \bar{U}_j \frac{\partial \bar{T}}{\partial x_j} = \frac{\nu}{Pr} \frac{\partial^2 \bar{T}}{\partial x_j \partial x_j} - \frac{\partial h_j}{\partial x_j}, \quad (4)$$

where an overbar indicates the filtered value. The effects of the unresolved SGS in the equations (2) to (4) appear in the SGS stress term τ_{ij} , SGS mass flux term q_{ij} , SGS heat flux term h_j , and filtered chemical reaction source term $\bar{\omega}$. These terms need to be modeled to represent the SGS effects by the filtered quantities at the resolved scales (GS). In this study, dynamic SGS models were employed to the SGS Reynolds stress and SGS mass and heat fluxes. For the filtered reaction source term, the SGS model developed in our previous study (Michioka *et al.*, 2001) was used.

MODELING FOR THE FILTERED REACTION SOURCE TERM

A second-order rapid reaction ($A + B \rightarrow P$) between acetic acid and ammonium hydroxide was used here. In such a rapid reaction, the timescale of the chemical reaction is far smaller than that of turbulent diffusion. This means that the time step Δt must be sufficiently smaller than the time scale of chemical reaction. However, such an extremely small time step cannot be treated even by a supercomputer. Therefore, the SGS model of Cook and Riley (1994) was modified to be applicable to a turbulent liquid flow with a rapid reaction. The model introduces a conserved scalar ζ and needs the SGS fluctuation of ζ . In liquid flows, the SGS fluctuation is not equal to the GS fluctuation because of its high Sc . To consider the SGS effect, the SGS fluctuation was assumed to be correlated with a test-scale fluctuation as

$$\bar{\zeta}'^2 \approx c_f \widetilde{\zeta}'^2, \quad (5)$$

where $\widetilde{\cdot}$ indicates the test-scale filtered value. The scale of the test filter was twice larger than the scale of the normal SGS filter. The correlation coefficient of $c_f = 5.0$ was obtained from the DNS of stationary isotropic liquid turbulence (Michioka *et al.*, 2001).

MODELING OF BUOYANCY EFFECT ON SGS FLOW FIELD

In a conventional dynamic SGS model for the SGS Reynolds stress, energy generation by shear is assumed to be equal to energy dissipation. From this assumption, we can derive

$$\tau_{ij} - \frac{1}{3} \delta_{ij} \tau_{kk} = -2C \bar{\Delta}^2 |\bar{S}| \bar{S}_{ij}. \quad (6)$$

Table 1: Computational conditions for a liquid mixing layer.

	U_0 [m/s]	ΔU [m/s] ($U_h - U_l$)	ΔT [K] ($T_h - T_l$)
neutral case	0.125	0.080	0
unstable case	0.125	0.080	-10
stable case	0.125	0.080	10

Table 2: Computational conditions for grid-generated turbulence.

	U_0 [m/s]	ΔT [K] ($T_h - T_l$)
neutral case	0.180	0
unstable case	0.180	-10
stable case	0.180	10

In the above equation, $\bar{S}_{ij} = (\frac{\partial \bar{U}_i}{\partial x_j} + \frac{\partial \bar{U}_j}{\partial x_i})/2$, and the coefficient C can be determined dynamically from GS quantities.

In stratified flows, the buoyancy may directly affect the SGS flow field. Especially in liquid flows, the buoyancy effect seems to be significant because of its high Pr . Wong and Lilly (1994) assumed that energy generation by shear and buoyancy is balanced with energy dissipation, and they derived

$$\begin{aligned} \tau_{ij} - \frac{1}{3} \delta_{ij} \tau_{kk} &= -2\nu_{SGS} \bar{S}_{ij} \\ &= -2C \bar{\Delta}^2 \left(1 + \frac{g_i \beta}{Pr_{SGS} |\bar{S}|^2} \frac{\partial \bar{T}}{\partial x_i} \right)^{\frac{1}{2}} |\bar{S}| \bar{S}_{ij}. \end{aligned} \quad (7)$$

By comparing the two LES predictions based on the above equations (6) and (7), the buoyancy effect on the SGS flow field will be discussed.

COMPUTATIONAL METHOD

The governing equations for the LES are given by equations (1) to (4). These equations were discretized on the staggered mesh arrangement to construct a finite-difference formation. The HSMAC method was used to solve the discretized equations. The second-order central difference method and the second-order Runge-Kutta method were used to calculate the spatial derivatives and the time integration, respectively.

The LES was carried out against two types of reacting liquid turbulent flows with thermal stratifications. One was a typical turbulent shear flow; a mixing layer, and the other was a typical isotropic turbulent flow; grid-generated turbulence.

MIXING LAYER. Figure 1 shows the schematic diagram of the computational domain for a mixing layer. In the neutral and stable cases, the computational domain was $480 \times 80 \times 80$ mm in the streamwise, vertical and spanwise directions and the numbers of grid points were $360 \times 60 \times 60$. In the unstable case, the mixing region being enlarged vertically, the domain was set to $480 \times 106 \times 80$ mm and the

number of grid points were set to $360 \times 80 \times 60$.

Table 1 shows the computational conditions for a mixing layer. The averaged streamwise velocity was set to 0.125m/s. The upper-layer streamwise velocity was set to 0.08m/s larger than the lower-layer one. In the unstable case, the upper-layer temperature was set to 10K lower than the lower-layer one. In the stable case, the upper-layer temperature was set to 10K higher than the lower-layer one.

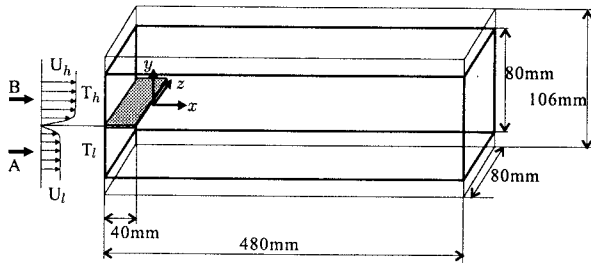


Figure 1: The computational domain for a mixing layer.

GRID-GENERATED TURBULENCE. Figure 2 shows the schematic diagram of the computational domain for grid-generated turbulence. The computational domain was $520 \times 80 \times 80$ mm and the number of grid points were $260 \times 80 \times 80$. The mesh size of a turbulence-generating grid, M , and the thickness of the square rod, d , were 2.0×10^{-2} m and 2.0×10^{-3} m, respectively. Table 2 shows the computational conditions for the grid-generated turbulence. The streamwise velocity was set to 0.180m/s. Under these conditions, the Reynolds number based on the mesh size (Re_M) was 4.0×10^3 . Bulk Richardson numbers (Ri_b) were 2.8×10^{-2} and -2.8×10^{-2} in stable and unstable cases, respectively.

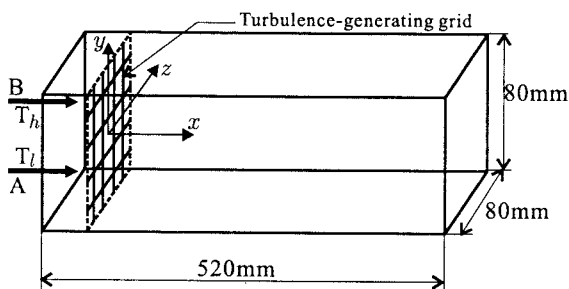


Figure 2: The computational domain for grid-generated turbulence.

RESULTS AND DISCUSSIONS

MIXING LAYER. Figure 3 shows the streamwise distributions of the mixing layer width δ_u in the velocity field. Two LES predictions are shown in the figure together with the measurements. Hereafter we refer the two LESs based on the equations (6) and (7) without and with buoyancy effect as LES(1) and LES(2), respectively. The both LES predictions are in good agreement with the measurements. In the neutral case, the mixing layer width grows linearly in the region of $x > 0.15$ m. This means that in neutral stratification a typical mixing layer is formed in the present LES.

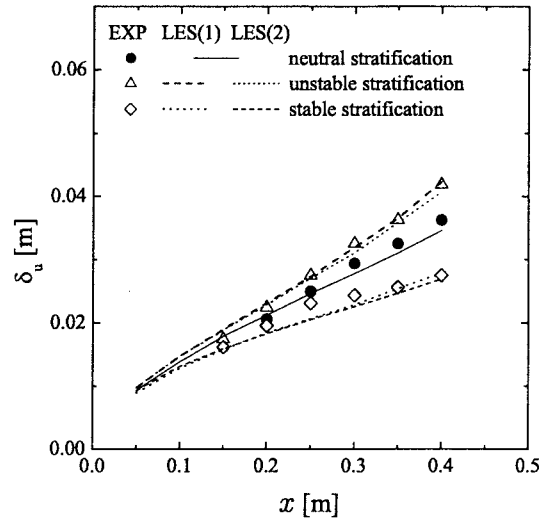


Figure 3: Streamwise distributions of the mixing layer width in the velocity field in a mixing layer.

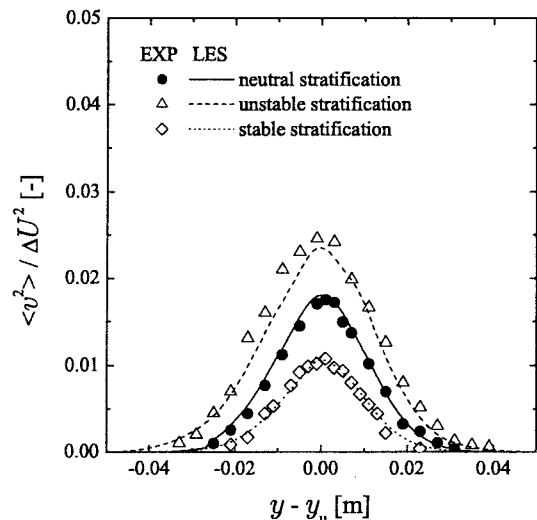


Figure 4: Vertical distributions of the turbulence intensities of vertical velocity fluctuation at $x=0.40$ m in a mixing layer.

The value of δ_u decreases in stable stratification, whereas δ_u increases in unstable stratification. Furthermore, it is found that in unstable and stable stratifications there is little difference in δ_u between the two predictions by LES(1) and LES(2). The little difference was also seen among other turbulent quantities. This means that the buoyancy does not affect directly on the SGS flow field and the SGS Reynolds stress (equation (6)) without buoyancy effect is applicable even to stratified flows. Therefore, the predictions only by LES(1) will be shown in the following figures.

Figure 4 shows the vertical distributions of the turbulence intensities of vertical velocity fluctuation at $x=0.40$ m.

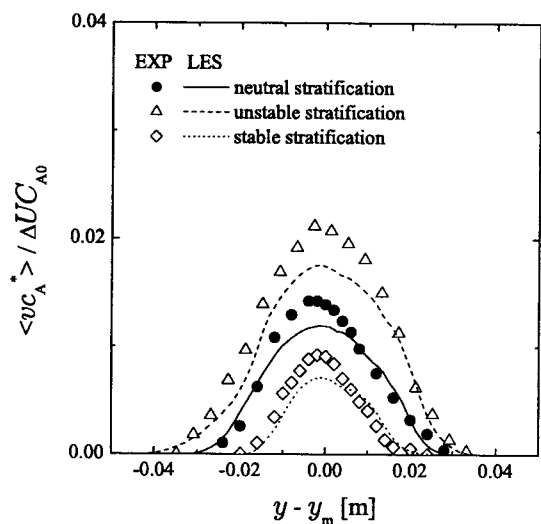


Figure 5: Vertical distributions of the vertical mass flux at $x=0.40\text{m}$ in a mixing layer.

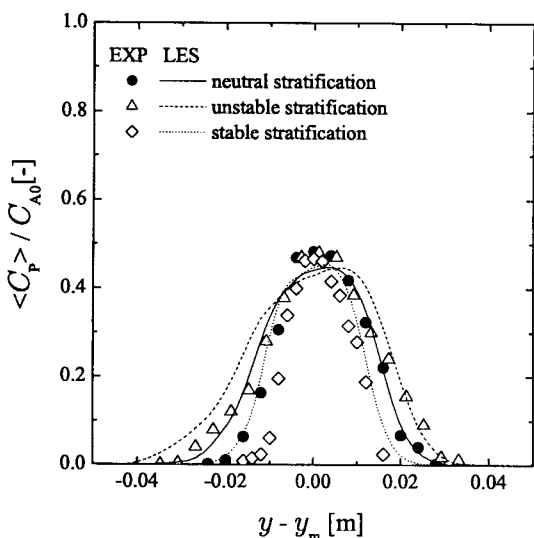


Figure 6: Vertical distributions of the mean concentration of chemical product at $x=0.40\text{m}$ in a mixing layer.

Here y_m is the vertical position with the mean velocity equivalent to the cross-sectional mean velocity. The promotion and suppression of turbulence can be seen in unstable and stable stratifications, respectively. The LES predictions are in good agreement with the measurements and the turbulence promotion and suppression by buoyancy are well predicted. These agreements between the LES predictions and the measurements in figures 3 and 4 show that the present LES can accurately predict the thermal stratification effects on the velocity field.

Figure 5 shows the vertical distributions of the vertical mass flux at $x=0.40\text{m}$. Here y_m is defined by the vertical position with the mean concentration of species A equivalent

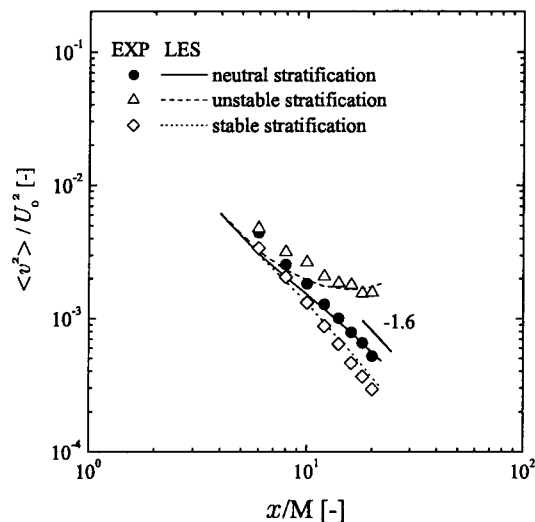


Figure 7: Streamwise distributions of the turbulence intensities of vertical velocity fluctuation in grid-generated turbulence.

to the cross-sectional mean concentration of species A. The mass transfer is promoted by unstable stratification and suppressed by stable stratification. The present LES can well estimate the buoyancy effects on the turbulent mass transfer. Figure 6 shows the vertical distributions of the mean concentration of chemical product at $x=0.40\text{m}$. The chemical reaction is also promoted by unstable stratification and is suppressed by stable stratification. Although there is a little difference between the predictions and measurements, the present LES well explains the measurements. These results show that the present LES can accurately estimate the buoyancy effects on the diffusive-reactive mechanism in the thermally-stratified mixing layer.

GRID-GENERATED TURBULENCE. Figure 7 shows the vertical distributions of the turbulence intensities of vertical velocity fluctuation on the center line ($y/M = z/M = 0$) in grid-generated turbulence. The intensity decays exponentially in neutral stratification and the exponent of -1.6 was close to the value of -1.4 obtained by Stapountzis *et al.* (1986). Although there is a little difference between the predictions and measurements in the upstream region of $x/M < 10$, the agreement is good in the downstream region. This means that in neutral stratification a typical isotropic grid-generated turbulence is formed in the present LES. In addition, the turbulence promotion and suppression by unstable and stable stratifications are well predicted. These results show that the present LES can well predict the thermally-stratified flow fields not only in the mixing layer but also in the grid-generated turbulence.

Figure 8 shows the vertical distributions of the vertical mass flux at $x/M=20$. The mass transfer is strongly affected by thermal stratifications as well as in the mixing layer. The present LES can well predict the thermal stratification effects on the turbulent mass transfer in the grid-generated turbulence. Figure 9 shows the vertical distributions of the mean concentration of chemical product at $x/M=20$. The

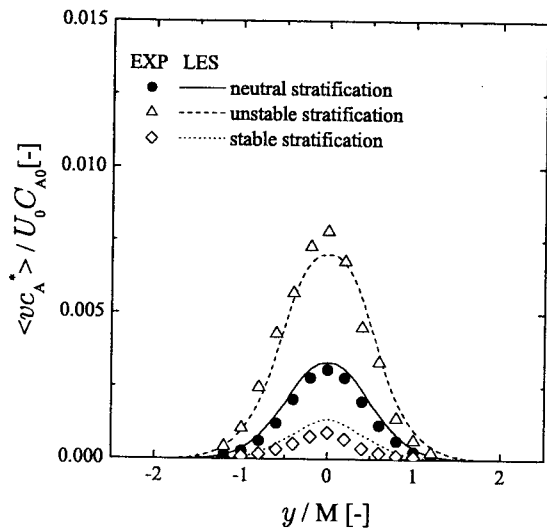


Figure 8: Vertical distributions of the vertical mass flux at $x/M=20$ in grid-generated turbulence.

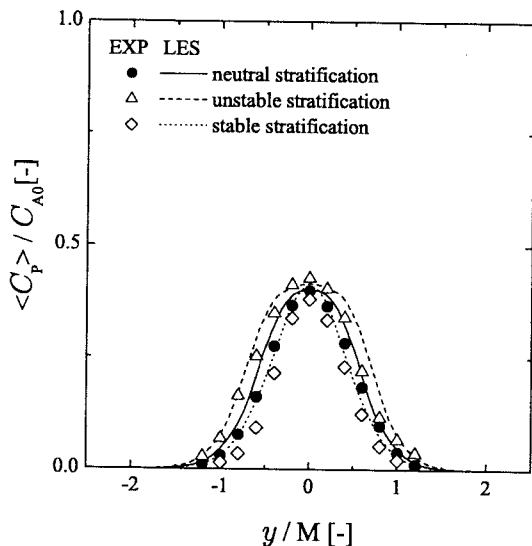


Figure 9: Vertical distributions of the mean concentration of chemical product at $x/M=20$ in grid-generated turbulence.

chemical reaction is promoted and suppressed by unstable and stable stratifications, respectively. The predictions are in good agreement with the measurements. These results also show that the present LES can accurately predict the buoyancy effects on the diffusive-reactive mechanism not only in the thermally-stratified mixing layer but also in the thermally-stratified grid-generated turbulence.

CONCLUSIONS

The present LES based on the SGS model proposed for the filtered chemical reaction source term was applied to

two types of thermally stratified reacting liquid turbulence; a mixing layer and grid-generated turbulence. The results from this study can be summarized as follows.

- The buoyancy effects induced by unstable and stable thermal stratifications on the SGS flow field are negligibly small even in liquid turbulent flows.
- The present LES can well predict the buoyancy effects and diffusive-reactive mechanism in thermally-stratified reacting liquid turbulence.

ACKNOWLEDGMENTS

This research was supported by the Ministry of Education, Science, Sports and Culture, Grant-in-Aid (No.14102016).

REFERENCES

- Cook, A. W. and Riley, J. J., 1994, "A subgrid model for equilibrium chemistry in turbulent flows", *Physics of Fluids*, Vol. 6, pp. 2868.
- Komori, S., Nagata, K., Kanzaki, T. and Murakami, Y., 1993, "Measurements of mass flux in a turbulent liquid flow with a chemical reaction", *AIChE J.*, Vol. 39, pp. 1611.
- Komori, S., Kanzaki, T. and Murakami, Y., 1994, "Concentration correlation in a turbulent mixing layer with chemical reactions", *J. Chem. Eng. Jpn.*, Vol. 27, pp. 742.
- Michioka, T., Onishi, R. and Komori, S., 2001, "Large Eddy Simulations of Turbulent Liquid Flows with Chemical Reactions", *Proceedings, 2nd International Symposium on Turbulence and Shear Flow Phenomena*, Vol. 3, pp. 321.
- Onishi, R., Michioka, T., Nagata, K. and Komori, S., 2003 "Effects of Thermal Stratifications on Turbulent Mixing and Chemical Reaction in Liquid Mixing Layer", *Trans. JSME. Ser. B.*, Vol.69, pp. 636 (in Japanese).
- Stapountzis, H., Sawford, B. L., Hunt, J. C. R. and Britter, R. E., 1986, "Structure of the Temperature Field Downwind of a Line Source in Grid Turbulence", *J. Fluid Mech.*, Vol. 165, pp. 401
- Wong, V. C. and Lilly D. K., 1994, "A comparison of two dynamic subgrid closure methods for turbulent thermal convection", *Phys. Fluids*, Vol. A6, pp. 1016

